Acta Biochim Biophys Sin 2023, 55(5): 769–782
https://doi.org/10.3724/abbs.2023087
Advance Access Publication Date: 8 May 2023
Original Article

Original Article

ATF1 promotes the malignancy of lung adenocarcinoma cells by transcriptionally regulating ZNF143 expression

Jinhong Mei[1,2,†], Yu Liu[1,2,†], Yiyun Sheng[1], Ying Liu[1,2], Limin Chen[3], Hailong Wang[3], Minzhang Cheng[3], Zhenyu Zhai[3], and Linlin Xu[1,2,*]

[1]Department of Pathology, the First Affiliated Hospital of Nanchang University, Nanchang 330006, China, [2]Institute of Molecular Pathology, Nanchang University, Nanchang 330006, China, and [3]Center for Experimental Medicine, the First Affiliated Hospital of Nanchang University, Nanchang 330006, China

[†]These authors contributed equally to this work.

*Corresponding address. Tel: +86-15879039389; E-mail: xulinlin@ncu.edu.cn

Received 9 November 2022 Accepted 29 December 2022

Abstract

The clinical oncogenic functions and mechanisms of activating transcription factor 1 (ATF1) in the progression of lung adenocarcinoma have not been completely elucidated. In this study, by employing human lung adenocarcinoma tissues and cells, we detect the correlation of ATF1 expression with the clinicopathological features and prognosis of patients with lung adenocarcinoma and find that ATF1 promotes lung adenocarcinoma cell proliferation and migration by transcriptionally enhancing zinc finger protein 143 (ZNF143) expression. ATF1 and ZNF143 are strongly expressed in lung adenocarcinoma tissues compared with those in the adjacent normal tissues, and high ATF1 and ZNF143 expressions are related to poor disease-free survival of lung adenocarcinoma patients. ATF1 overexpression results in increased proliferation and migration of lung adenocarcinoma cells, whereas knockdown of *ATF1* inhibits cell proliferation and migration. Furthermore, ATF1 transcriptionally regulates the expression of ZNF143, and ATF1 and ZNF143 expressions are positively correlated in lung adenocarcinoma tissues. *ZNF143* knockdown blocks lung adenocarcinoma cell migration, which is mediated by ATF1 upregulation. Hence, this study provides a potential therapeutic candidate for the treatment of lung adenocarcinoma.

Key words activating transcription factor 1, zinc finger protein 143, cell proliferation, cell migration, lung adenocarcinoma

Introduction

Lung cancer is one of the most frequently diagnosed cancers and the leading cause of cancer-related deaths in the world [1]. Non-small cell lung cancer (NSCLC) accounts for approximately 85% of all lung cancer cases, among which lung adenocarcinoma accounts for 78% of NSCLC cases, and is the principal subtype [2]. Currently, surgery concurrent chemoradiotherapy and immunotherapy have been reported to increase the survival rate of lung adenocarcinoma patients. However, recurrence and chemotherapy resistance are the major obstacles to reducing the mortality of lung adenocarcinoma. Thus, elucidating the mechanisms underlying the pathogenesis and progression of lung adenocarcinoma is highly necessary to find new therapeutic targets against lung adenocarcinoma.

Activating transcription factor 1 (ATF1), a leucine zipper transcription factor, binds to the consensus ATF/cAMP response element (CRE) site 'TGACGTCA' of target genes and is a member of the ATF/CREB family [3]. Numerous publications have reported that ATF1 transcriptionally regulates the expressions of target genes to mediate various cellular processes, and the effects of ATF1 on the progression of tumors (including lung cancer, colorectal cancer, and nasopharyngeal carcinoma) have been gradually disclosed [3–7]. In lung cancer cells, ATF1 promotes cell migration and invasion by regulating the expressions of EGFR and MMP-2 [4]. Targeting ATF1 with miR-30a regulates the radiosensitivity of NSCLC cells [5]. However, the clinical significance of ATF1 in lung adenocarcinoma is unknown, and the oncogenic role and mechanism of ATF1 in the progression of lung adenocarcinoma remain poorly understood.

Zinc finger protein 143 (ZNF143) is a transcription factor that positively regulates many cell cycle- and DNA replication-related genes [8]. ZNF143 is closely related to the progression of various tumors, including lung adenocarcinoma [9]. Although ZNF143 is

strongly expressed in lung adenocarcinoma [9], the mechanism remains to be disclosed.

In the present study, we found that ATF1 was highly expressed in lung adenocarcinoma tissues, and high levels of ATF1 and ZNF143 were associated with the recurrence of lung adenocarcinoma. Upregulation of ATF1 increased the proliferation and migration of lung adenocarcinoma cells, whereas knockdown of *ATF1* resulted in inhibition of cell proliferation and migration. Furthermore, we found that ATF1 transcriptionally regulated ZNF143 expression. Moreover, downregulation of ZNF143 expression rescued ATF1 overexpression and increased lung adenocarcinoma cell migration, and ATF1 and ZNF143 were positively correlated in lung adenocarcinoma tissues. Hence, this study elucidated the role and mechanism of ATF1 in the progression of lung adenocarcinoma, potentially providing a novel therapeutic target for lung adenocarcinoma treatment and a mechanism for the high expression of ZNF143 observed in lung adenocarcinoma tissues.

Materials and Methods

Bioinformatics analysis

The prognosis of lung adenocarcinoma patients was assessed using the TCGA-LUAD and GEO-LUAD datasets, and validated through Kaplan-Meier plots available on kmplot.com (10.1371/journal.pone.0082241, 10.1038/s41598-021-84787-5). The DNA binding site of ATF1 was obtained from MotifMap (10.1186/1471-2105-12-495), while the high-throughput ChIP-Seq analysis of ATF1 binding to the promoter region was conducted by the ENCODE project (10.1038/s41586-020-2528-x) and visualized through Genome Browser (10.1101/gr.229102). Furthermore, cBioPortal was utilized to analyze and visualize the correlation between the expression of ATF1 and ZNF143 in lung adenocarcinoma tissues within the TCGA-LUAD dataset (10.1126/scisignal.2004088).

Human tissue specimens

Human primary lung adenocarcinoma tissues and paired adjacent normal tissues without prior radiotherapy or chemotherapy were obtained by surgical intervention. All samples had complete clinical data and were collected at the First Affiliated Hospital of Nanchang University (Nanchang, China). The diagnosis of lung adenocarcinoma was made according to HE staining. Detailed clinical and pathological information of the patients is summarized in Table 1. The study protocol was approved by the Institutional Review Board of the First Affiliated Hospital of Nanchang University [(2022) Medical Research Council Quick Review No. 3-026].

Immunohistochemistry (IHC) staining of human tissue specimens

IHC staining of ATF1 and ZNF143 was performed as described

Table 1. Association of ATF1 and ZNF143 expression levels with different clinicopathologic characteristics in lung adenocarcinoma

Clinicopathologic characteristic	ATF1 expression		*P*	ZNF143 expression		*P*
	Low	High		Low	High	
Sex						
Male	50 (21%)	69 (29%)	0.051	59 (25%)	60 (25%)	0.237
Female	64 (27%)	53 (22%)		67 (28%)	50 (21%)	
Age, year						
<60	56 (24%)	54 (23%)	0.454	56 (24%)	54 (23%)	0.475
≥60	58 (25%)	68 (29%)		70 (30%)	56 (24%)	
Smoke						
No	71 (30%)	65 (28%)	0.162	73 (31%)	63 (27%)	0.918
Yes	43 (18%)	57 (24%)		53 (22%	47 (20%)	
Tumor size						
≤3 cm	80 (34%)	66 (28%)	0.011	76 (32%)	70 (30%)	0.601
>3 cm	34 (14%)	56 (24%)		50 (21%)	40 (17%)	
Degree of differentiation						
Well	65 (28%)	9 (4%)	<0.001	51 (22%)	23 (10%)	<0.001
Moderately	29 (12%)	70 (30%)		55 (23%)	44 (19%)	
Poor	20 (8%)	43 (18%)		20 (8%)	43 (18%)	
T factor						
T1	81 (34%)	65 (28%)	0.015	77 (33%)	69 (29%)	0.249
T2	26 (11)	40 (17%)		40 (17%)	26 (11%)	
T3	6 (3%)	9 (4%)		5 (2%)	10 (4%)	
T4	1 (0%)	8 (3%)		4 (2%)	5 (2%)	
Lymph node metastasis (N factor)						
N0	81 (34%)	74 (31%)	0.076	81 (34%)	74 (31%)	0.387
N1	24 (10%)	25 (11%)		29 (12%)	20 (8%)	
N2	9 (4%)	21 (9%)		16 (7%)	14 (6%)	
N3	0 (0%)	2 (1%)		0 (0%)	2 (1%)	

(*Continued*)

Clinicopathologic characteristic	ATF1 expression		*P*	ZNF143 expression		*P*
	Low	High		Low	High	
Distant invasion (M factor)						
No	89 (38%)	81 (34%)	0.046	98 (42%)	72 (31%)	0.035
Yes	25 (11%)	41 (17%)		28 (12%)	38 (16%)	
Vascular invasion						
No	108 (46%)	110 (47%)	0.186	118 (50%)	100 (42%)	0.429
Yes	6 (3%)	12 (5%)		8 (3%)	10 (4%)	
Neural invasion						
No	112 (47%)	118 (50%)	0.457	123 (52%)	107 (45%)	0.866
Yes	2 (1%)	4 (2%)		3 (1%)	3 (1%)	
Clinical stage						
Stage I	66 (28%)	47 (20%)	0.021	65 (28%)	48 (20%)	0.218
Stage II	13 (6%)	15 (6%)		16 (7%)	12 (5%)	
Stage III	10 (4%)	19 (8%)		17 (7%)	12 (5%)	
Stage IV	25 (11%)	41 (17%)		28 (12%)	38 (16%)	
Radiotherapy						
No	99 (42%)	102 (43%)	0.383	108 (46%)	93 (39%)	0.687
Yes	14 (6%)	20 (8%)		17 (7%)	17 (7%)	
Chemotherapy						
No	62 (26%)	67 (28%)	0.935	64 (27%)	65 (28%)	0.202
Yes	52 (22%)	55 (23%)		62 (26%)	45 (19%)	

Note: clinicopathologic characteristics that significantly associated with ATF1 or ZNF143 levels were marked as red, and that might be related to ATF1 or ZNF143 levels were marked as blue.

previously [10]. The expression levels of ATF1 and ZNF143 in each specimen were scored according to the intensity of cytoplasmic staining (no staining = 0, weak staining = 1, moderate staining = 2, and strong staining = 3) and the extent of stained cells (0% = 0, 1%–24% = 1, 25%–49% = 2, 50%–74% = 3, and 75%–100% = 4). The immunoreactive scores indicating the expression levels of ATF1 and ZNF143 were obtained by multiplying the intensity score by the extent score. To distinguish lung adenocarcinoma tissues from the adjacent normal tissues, consecutive sections were stained with hematoxylin and eosin (HE).

Western blot analysis

Human tissue specimen lysates were prepared with RIPA buffer containing a protease inhibitor cocktail, and the concentration of protein was measured using a BCA protein assay kit (Thermo Scientific, Waltham, USA). The lysate containing 100 μg of protein was separated by SDS-PAGE and then transferred to nitrocellulose membranes (Millipore, Billerica, USA). After being blocked, membranes were incubated with primary antibodies, followed by incubation with horseradish peroxidase-conjugated secondary antibodies. The anti-ATF1 antibody was obtained from Proteintech (#11946-1-AP; Chicago, USA), anti-ZNF143 antibody was obtained from Sigma (#HPA003263; St Louis, USA), and anti-GAPDH antibody was purchased from Cell Signaling Technology (#5174; Beverly, USA). The secondary antibodies were purchased from Thermo Scientific [anti-rabbit IgG (H + L) antibody, #31460; anti-mouse IgG (H + L) antibody, #31430]. Finally, the protein bands were visualized using Western ECL Substrate (#170-5060; Bio-Rad, Hercules, USA) and the band intensity was determined with ImageJ software (NIH, Bethesda, USA), and the expression levels of ATF1 and ZNF143 were normalized to GAPDH. GAPDH was used as the loading control.

Cell culture

The human lung adenocarcinoma cell line A549, PC9, NCI-H1975, and NCI-H1299 was obtained from American Type Culture Collection (ATCC; Manassas, USA). Cells were cultured in a humidified incubator with 5% CO_2 at 37°C, as recommended by the supplier.

Cell transfection and lentivirus infection

Transient transfection of NCI-H1299 cells was performed using polyethylenimine (Sigma). NCI-H1299 cells with stable overexpression or knockdown of *ATF1* were generated using a lentiviral expression system (Invitrogen, Carlsbad, USA). In all experiments, the medium was replaced every two days.

The Lenti-ATF1 construct (pHAGE-CMV-ATF1-IZsGreen) for ATF1 overexpression and Lenti-shRNA-ATF1 construct (pSUPERretro) for *ATF1* knockdown were generated, packed, and purified by ultracentrifugation (50,000 *g* at 4°C for 2 h). NCI-H1299 cells (in a 6-well plate) were transduced with the purified lentivirus for 12–16 h. The shRNA target sequences of *ATF1* were as follows: shRNA-ATF1#280, 5′-AGCAATATGAGAAATGTGAGC-3′; shRNA-ATF1#1853, 5′-TTAAGGGCCTGTAAACATTCC-3′; and shRNA-ATF1#280 was used to generate lentivirus for downregulating ATF1 expression. The shRNA target sequence of ZNF143 was 5′-GCTACAAGAGTAACTGCTAAA-3′. A control shRNA (shNC; 5′-GATCATACGTGCGATCAGA-3′) was used as the negative control.

Cell proliferation assay

A plate colony formation assay was performed to evaluate cell proliferation. Briefly, 1000 cells were seeded into 6-well plates and incubated with medium containing 10% FBS for two weeks. Then, the cells were fixed with 4% paraformaldehyde (PFA) and stained with crystal violet solution. A microscopic imaging system was employed to take photos. The number of colonies was determined using ImageJ software (NIH). The experiments were repeated at least three times.

Cell migration assay

Cell migration ability was detected by using Transwell assay without precoated Matrigel. Briefly, 100 μL of medium containing 1% FBS with 3×10^4 cells was seeded into the upper chambers, and 600 μL of growth medium supplemented with 10% FBS was added into the bottom wells. After incubation for 24 h, the cells on the lower surface of the membrane were fixed with 4% PFA and stained with crystal violet. Images were taken using a microscopic imaging system. The number of migrating cells was counted in each field using ImageJ software (NIH), and at least 4 fields were counted for each sample. The experiments were repeated three times.

Real-time PCR assay

Total RNA of cells was extracted using Trizol reagent (Life Technologies, Carlsbad, USA) according to the manufacturer's instructions, and 1 μg of total RNA was reverse transcribed into cDNA using One Step PrimeScript miRNA cDNA Synthesis kit (#D350A; TaKaRa, Dalian, China). Real-time PCR assays were carried out uisng TB Green Premix Ex *Taq* II (RR820A) on an ABI StepOnePlus Real-Time PCR System (Applied Biosystem, Foster City, USA). The following primers were used: *ATF1*-forward, 5′-GACTCATCCGACAGCATAGG-3′ and *ATF1*-reverse, 5′-TTCTCCGTCTCCTTTTCTGC-3′; *ZNF143*-forward, 5′-CGAGCAGGAAGCCTTCTTTGA-3′ and *ZNF143*-reverse, 5′-CGTAATCTGGGACCCTTTAAGAAC-3′; and *GAPDH*-forward, 5′-ACATCGCTCAGACACCATG-3′ and *GAPDH*-reverse, 5′-TGTAGTTGAGGTCAATGAAGGG-3′. The gene expression levels were calculated using the $2^{-\Delta\Delta CT}$ method, and GAPDH was used as the internal control.

Xenograft mouse model

The A549 cells were infected with ATF1-overexpressing and control lentivirus respectively to generate ATF1-upregulated A549 cells (Lv-ATF1) or control A549 cells (Lv-Con). A 200 μL of Lv-ATF1 cell suspension (8×10^6 cells) or 200 μL of Lv-Con cell suspension (8×10^6 cells) were injected subcutaneously into the two flanks of 5- to 6-week-old Balb/c-nu mice (National Resource Center for Mutant Mice, Nanjing, China). The tumor volume was measured every two days with a caliper and quantified using the following formula: tumor volume = length (mm) × width^2 (mm^2)/2. At the end of experiment, mice were anesthesia and executed, and tumor tissues were collected for subsequent HE staining and IHC analysis using antibodies against ATF1 (#11946-1-AP; Proteintech), ZNF143 (#HPA003263; Sigma), Ki67 (#ZM-0167; ZSGB-Bio, Beijing, China), MMP7 (#AF0218; Affinity Biosciences, Changzhou, China) and MMP9 (#10375-2-AP; Proteintech). The animal experiment was approved by the Institutional Review Board of the First Affiliated Hospital of Nanchang University [(2022) Medical Research Council Quick Review No. 3-026].

Statistical analysis

Data are shown as the mean ± SD from at least three independent experiments. The expressions of ATF1 and ZNF143 in lung adenocarcinoma tissues and paired adjacent normal tissues were statistically analyzed using unpaired Student's *t* test. The difference in the cell migration ratio was assessed by unpaired Student's *t* test. Differences were considered significant if $P < 0.05$. All statistical analyses were carried out using SPSS v.13.0 software (SPSS Inc., Chicago, USA).

Results

High level of ATF1 is related to poor prognosis in lung adenocarcinoma patients

To evaluate whether ATF1 is correlated with the development and progression of lung adenocarcinoma, we first detected the expression level of ATF1 in lung adenocarcinoma tissues. A total of 236 paired human primary lung adenocarcinoma tissues and adjacent normal tissues were collected and subject to immunohistochemistry and western blot analysis. As shown in Figure 1A–C, ATF1 was highly expressed in lung adenocarcinoma tissues compared with that in normal tissues. In 8 paired randomly selected human primary lung adenocarcinoma tissues and adjacent normal tissues, the high expression of ATF1 in lung adenocarcinoma tissues was confirmed by western blot analysis (Figure 1D). Scores of 0 to 12 were used to evaluate the expression of ATF1. A score less than the mean indicates low expression, and a score greater than the mean indicates high expression. High expression of ATF1 was strongly correlated with tumor size ($P = 0.011$), tumor cell differentiation ($P < 0.001$), tumor TNM stage (T factor, $P = 0.015$; N factor, $P = 0.076$; M factor, $P = 0.046$), and clinical stage ($P = 0.021$) (Table 1). Univariate and multivariate analyses were performed to estimate the factors associated with the recurrence and survival of lung adenocarcinoma patients. The results showed that high expression of ATF1 was associated with disease-free survival (Table 2). We further analyzed the relationship of the expression level of ATF1 with the survival rate of patients with lung adenocarcinoma using the Kaplan-Meier method and found that lung adenocarcinoma patients with high level of ATF1 had poor disease-free survival rates, whereas the relationship between ATF1 expression and overall survival rate was weak in our clinical cohort (Figure 1E,F). Furthermore, based on the TCGA dataset, we found that patients with higher expression of ATF1 displayed a poorer prognosis than those with lower expression of ATF1 (Figure 1G). The correlation between high expression level of ATF1 and poorer prognosis of lung adenocarcinoma was confirmed by the GEO dataset (Figure 1H). Hence, these results demonstrated that ATF1 is highly associated with the pathological progression of lung adenocarcinoma.

Upregulation of ATF1 promotes the malignancy of lung adenocarcinoma cells

To investigate the oncogenic role of ATF1 in lung adenocarcinoma, the expression levels of ATF1 in various lung adenocarcinoma cell lines were detected by western blot analysis (Figure 2A). A549 cells expressing lower levels of ATF1 were chosen to infect ATF1-overexpressing and control lentivirus to generate ATF1-upregulated (Lv-ATF1) and corresponding control (Lv-Con) cells. The *ATF1* mRNA levels in these cell lines were determined by real-time PCR assay (Figure 2B). As shown in Figure 2C, upregulation of

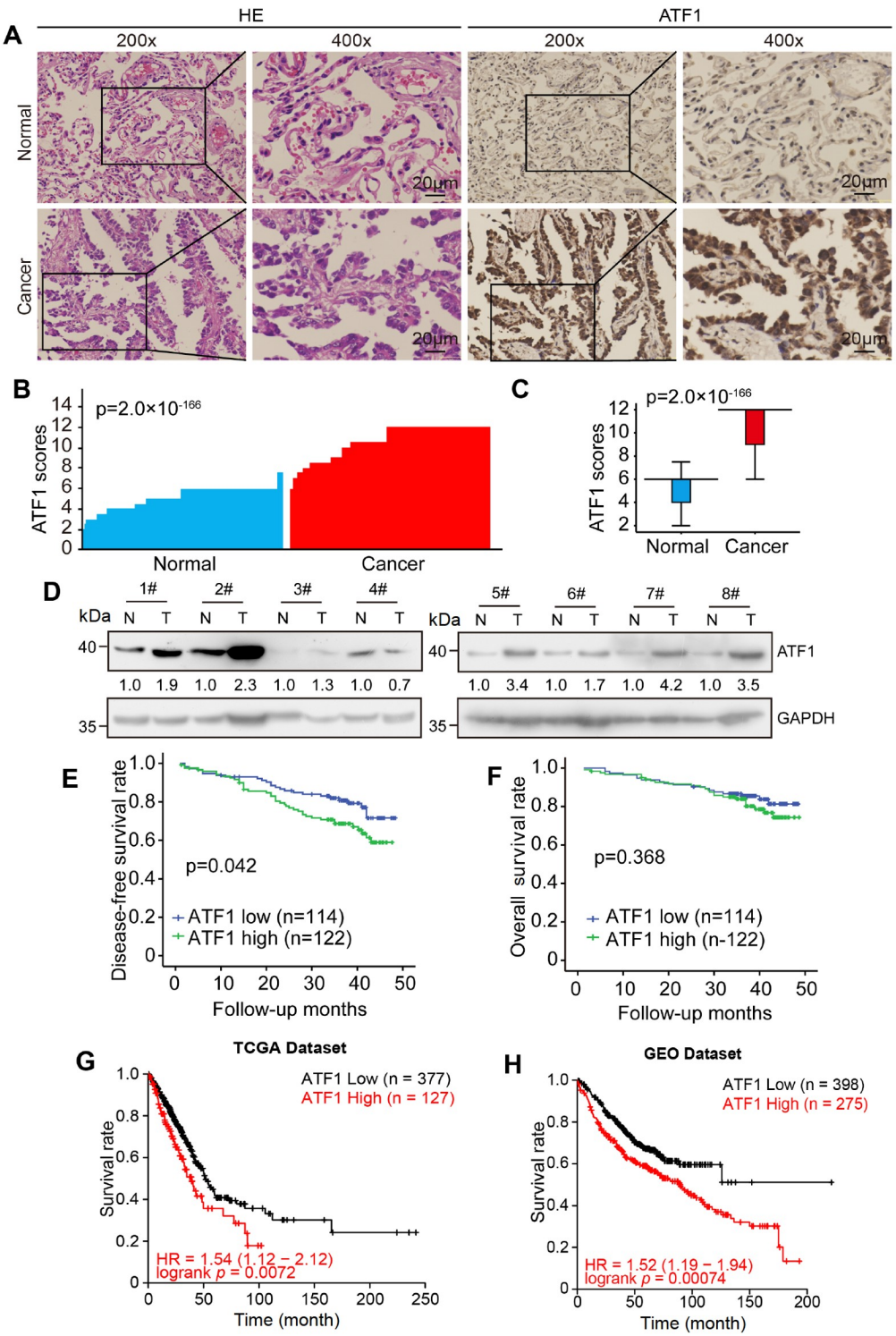

Figure 1. High ATF1 level is correlated with poor prognosis of lung adenocarcinoma ATF1 was upregulated in lung adenocarcinoma tissues compared with adjacent normal tissues, as detected by IHC. (A) Representative images with magnified local images showing detailed information are presented. (B) ATF1 scores for each lung adenocarcinoma and adjacent tissue were plotted. (C) Box plots of the scores of ATF1 expression in lung adenocarcinoma and adjacent tissues are shown. The *P* value was determined by independent-sample t test, n = 236. (D) ATF1 was highly expressed in lung adenocarcinoma tissues. Proteins extracted from lung adenocarcinoma and paired normal tissues from 8 patients were subjected to western blot analysis. N, adjacent normal tissue; T, lung adenocarcinoma tissue. (E) Lung adenocarcinoma patients with high ATF1 expression had a poor disease-free survival rate in our clinical cohort. The *P* values were determined using the log-rank (Mantel-Cox) test. (F) High expression of ATF1 had no significant effect on overall survival in our clinical cohort. The *P* values were determined using the log-rank (Mantel-Cox) test. (G–H) High ATF1 level is correlated with poor survival of patients with lung adenocarcinoma by analyzing data from TCGA and GEO datasets. Univariate analysis was performed to analyze the survival rate of patients with lung adenocarcinoma.

Table 2. Univariate and multivariate analysis of factors associated with recurrence and survival of lung adenocarcinoma patients

	Disease-free survival								Overall survival							
	Univariate analysis			*P*	Multivariate analysis			*P*	Univariate analysis			*P*	Multivariate analysis			*P*
	HR	95% CI			HR	95% CI			HR	95% CI			HR	95% CI		
		Lower	Upper			Lower	Upper			Lower	Upper			Lower	Upper	
Sex (male versus female)	0,774	0.476	1.260	0.303					0.863	0.473	1.572	0.629				
Age (<60 versus ≥60)	0.598	0.366	0.976	0.040	0.782	0.434	1.410	0.414	1.774	0.947	3.321	0.073				
Smoke (no versus yes)	1.167	0.719	1.895	0.532					1.420	0.781	2.583	0.250				
Tumor size (≤3 versus >3cm)	2.543	1.560	4.146	<0.001	1.001	0.381	2.627	0.998	1.917	1.052	3.494	0.034	0.841	0.437	1.618	0.605
Differentiation (well, moderately, poor)	2.041	1.464	2.844	<0.001	1.015	0.586	1.758	0.959	2.490	1.612	3.846	<0.001	1.608	0.919	2.814	0.096
T factor (T1, T2, T3, T4)	1.506	1.168	1.941	0.002	1.168	0.662	2.061	0.592	1.373	0.987	1.909	0.060				
Lymph node metastasis (N factor, N0, N1, N2, N3)	1.937	1.465	2.561	<0.001	1.098	0.740	1.630	0.642	2.411	1.740	3.339	<0.001	1.584	1.038	2.417	0.033
Distant invasion (M factor, no versus yes)	35.422	16.802	74.679	<0.001	3.645	0.589	22.558	0.164	6.639	3.460	12.737	<0.001	1.332	0.316	5.622	0.696
Vascular invasion (no versus yes)	3.658	1.906	7.021	<0.001	1.836	0.791	4.262	0.157	1.830	0.720	4.654	0.205				
Neural invasion (no versus yes)	3.122	0.974	10.006	0.055	1.417	0.340	5.900	0.632	1.916	0.463	7.925	0.369				
Clinical stage (stage I, II, III, IV)	5.629	3.605	8.789	<0.001	3.014	1.188	7.648	0.020	2.499	1.829	3.415	<0.001	2.135	1.006	4.530	0.048
Radiotherapy (no versus yes)	5.232	3.181	8.604	<0.001	1.287	0.683	2.424	0.434	2.548	1.324	4.906	0.005	0.924	0.432	1.975	0.839
Chemotherapy (no versus yes)	4.162	2.394	7.236	<0.001	0.832	0.382	1.813	0.643	2.231	1.191	4.177	0.012	0.606	0.275	1.335	0.214
ATF1 expression (low versus high)	1.663	1.011	2.734	0.045	1.084	0.576	2.040	0.802	1.319	0.720	2.418	0.371				
ZNF143 expression (low versus high)	1.933	1.179	3.168	0.009	2.033	1.067	3.873	0.031	1.078	0.593	1.962	0.805				

Note: clinicopathologic characteristics that significantly associated with ATF1 or ZNF143 levels were marked as red.

ATF1 increased the clone number of A549 cells compared with the control cells. Additionally, ATF1-overexpressing A549 cells grew faster than the control cells (Figure 2D). Upregulation of ATF1 expression promoted the migration ability of A549 cells (Figure 2E). Furthermore, ATF1 was also overexpressed in NCI-H1299 cells, which harbored moderate expression levels of ATF1 compared with other lung adenocarcinoma cell lines. The mRNA expression of *ATF1* was detected by real-time PCR assay (Figure 2F), and overexpression of *ATF1* drastically promoted the cell migration ratio compared with the control cells (Figure 2G). Therefore, these results indicated that upregulation of ATF1 expression promoted the malignancy of lung adenocarcinoma cells.

Downregulation of ATF1 decelerates the proliferation and migration of lung adenocarcinoma cells

To investigate the effects of *ATF1* knockdown on the malignancy of lung adenocarcinoma cells, we stably downregulated the expression of ATF1 in NCI-H1299 cells with the lentivirus system to generate ATF1-downregulated cells (Lv-shATF1) and corresponding control cells (Lv-shNC), and real-time PCR data confirmed the significantly decreased expression of *ATF1* (Figure 3A). Knockdown of *ATF1* decreased the clone number and markedly inhibited the cell migration ratio (Figure 3B,C). Furthermore, PC9 cells that expressed higher level of ATF1 were chosen for infection with an ATF1-knockdown lentivirus to knock down the expression of ATF1 (Figure 3D). Downregulation of ATF1 expression inhibited the proliferation and migration of PC9 cells (Figure 3E,F). To confirm the effects of *ATF1* knockdown on the inhibition of the cell phenotype in lung adenocarcinoma, ATF1 overexpression was performed in NCI-H1299 Lv-shATF1 and corresponding control cells. The results demonstrated that ATF1 overexpression rescued ATF1 downregulation-mediated inhibition of cell migration (Figure 3G,H). Taken together, these data demonstrated that ATF1 plays a key role in the proliferation and migration of lung adenocarcinoma cells.

ATF1 transcriptionally regulates ZNF143 expression

To explore the mechanism by which ATF1 is involved in the pathological process of lung adenocarcinoma, we investigated the downstream target genes transcriptionally regulated by ATF1. By analyzing the transcription factor ChIP-seq clusters from the ENCODE database, we found that ATF1 might transcriptionally

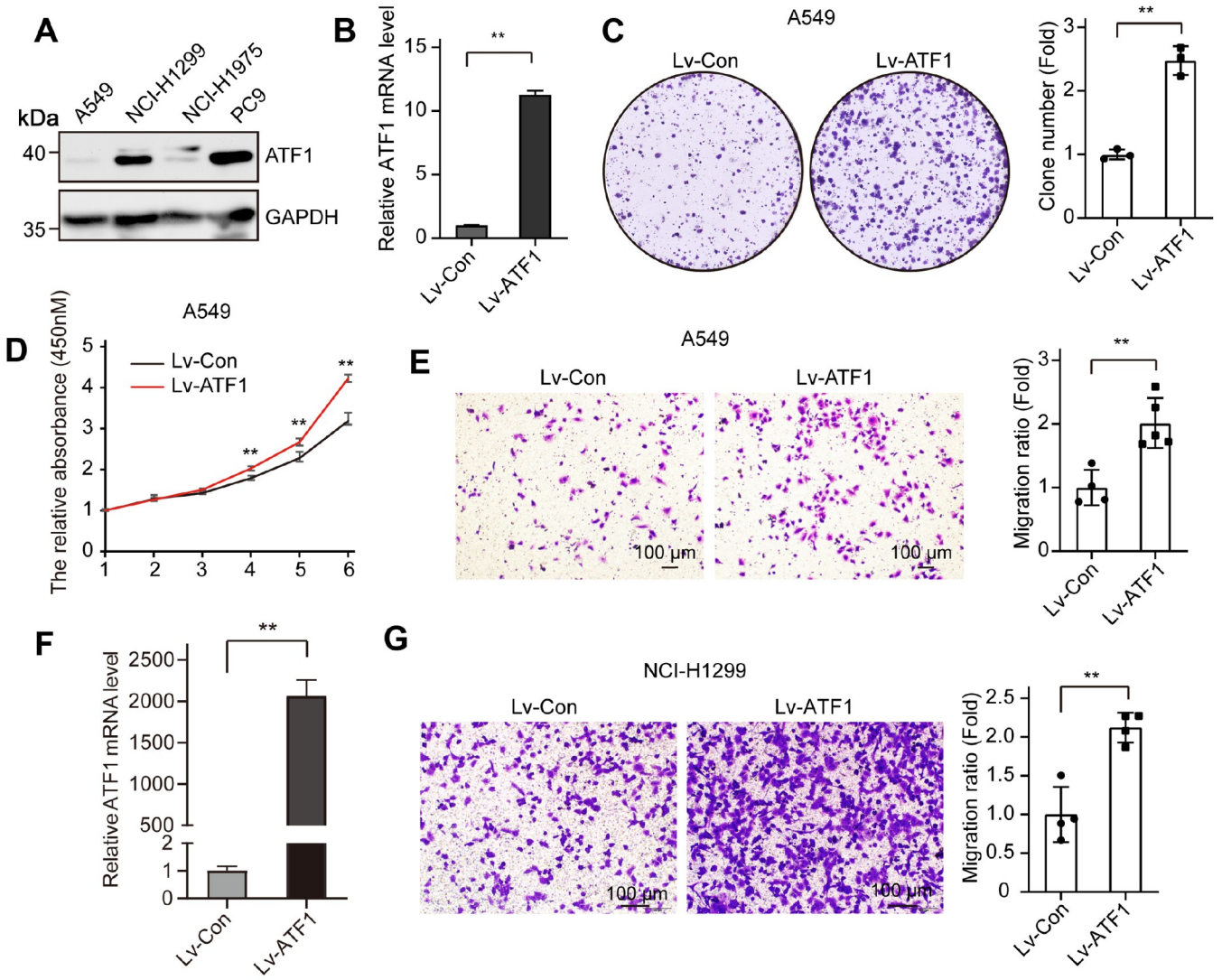

Figure 2. ATF1 overexpression promotes lung adenocarcinoma cell proliferation and migration (A) The expression of ATF1 in various lung adenocarcinoma cells was detected by western blot analysis. (B) ATF1 was stably upregulated in A549 cells, as determined by real-time PCR. (C) Upregulation of ATF1 expression enhanced the proliferation of A549 cells. (D) Overexpression of ATF1 promoted the growth of A549 cells. (E) Upregulation of ATF1 expression resulted in an increase in A549 cell migration. (F) ATF1 was stably overexpressed in NCI-H1299 cells. NCI-H1299 cells were infected with control and ATF1 overexpression lentiviruses, and the expression of ATF1 was determined by real-time PCR. (G) Overexpression of ATF1 promoted the migration of NCI-H1299 cells. Quantification of the cell migration ratio was carried out. Data are presented as the mean ± SD. $^{**}P < 0.01$.

regulate the expression of ZNF143, given that ATF1 was predicted to bind to the promoter of the *ZNF143* gene (Figure 4A). According to the conserved binding sequence of ATF1 (Figure 4B), we identified four potential binding sites of ATF1 in the promoter of the *ZNF143* gene (Figure 4C). Moreover, there was a strong correlation between the mRNA levels of *ATF1* and *ZNF143* in lung adenocarcinoma through analyzing in the cBioPortal database (Figure 4D). The lung adenocarcinoma cell line NCI-H1299 transfected with a plasmid that overexpressed ATF1 exhibited higher expression level of ZNF143 than control cells (Figure 4E). In contrast, NCI-H1299 cells were transfected with a plasmid that expressed ATF1 shRNA to downregulate the expression of ATF1, and knockdown of *ATF1* inhibited the expression of ZNF143 (Figure 4F). Moreover, overexpression of ATF1 enhanced the expression of ZNF143 in lung adenocarcinoma cells, whereas downregulation of ATF1 expression reduced the expression of ZNF143 in lung adenocarcinoma cells (Figure 4G,H). Altogether, these results showed that the expression of ZNF143 was transcriptionally regulated by ATF1.

ATF1 promotes the migration of lung adenocarcinoma cells by regulating ZNF143 expression

To detect whether ATF1 promotes the migration of lung adenocarcinoma cells through ZNF143, we determined the effect of ZNF143 on the migration of lung adenocarcinoma cells. In lung adenocarcinoma cells, knockdown of *ZNF143* inhibited cell migration (Figure 5A,B). Furthermore, we downregulated ZNF143 expression in ATF1-overexpressing lung adenocarcinoma cells by infection with ZNF143-knockdown lentivirus, and knockdown of *ZNF143* blocked ATF1 overexpression-mediated increases in cell

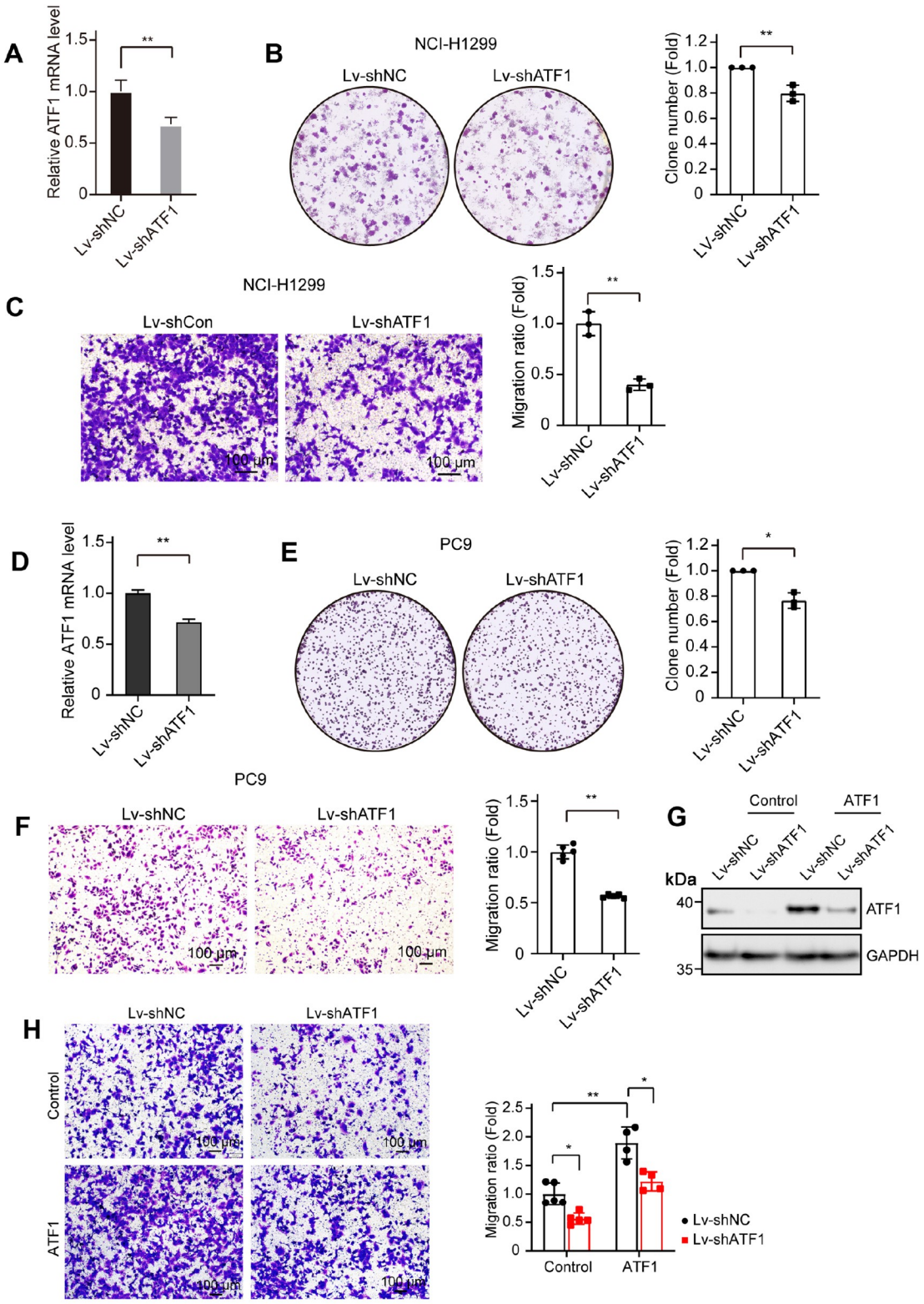

Figure 3. Downregulation of ATF1 expression inhibits the proliferation and migration of lung adenocarcinoma cells (A) ATF1 expression was stably downregulated in NCI-H1299 cells. NCI-H1299 cells were infected with control (Lv-shNC) or ATF1 knockdown (Lv-shATF1) lentiviruses, and ATF1 expression was detected by real-time PCR. (B) Downregulation of ATF1 expression led to a decrease in the clone number of NCI-H1299 cells. (C) Knockdown of *ATF1* inhibited NCI-H1299 cell migration. The cell migration ratio was quantified. (D) ATF1 was stably knocked down in PC9 cells, as determined by real-time PCR. (E) The clone number was decreased in *ATF1*-knockdown PC9 cells. (F) Downregulation of ATF1 expression decelerated the migration of PC9 cells. (G) ATF1 expression levels were detected by western blot analysis. (H) Overexpression of ATF1 rescued *ATF1* knockdown-mediated inhibition of H1299 cell migration. Data are presented as the mean ± SD. $*P < 0.05$, $**P < 0.01$.

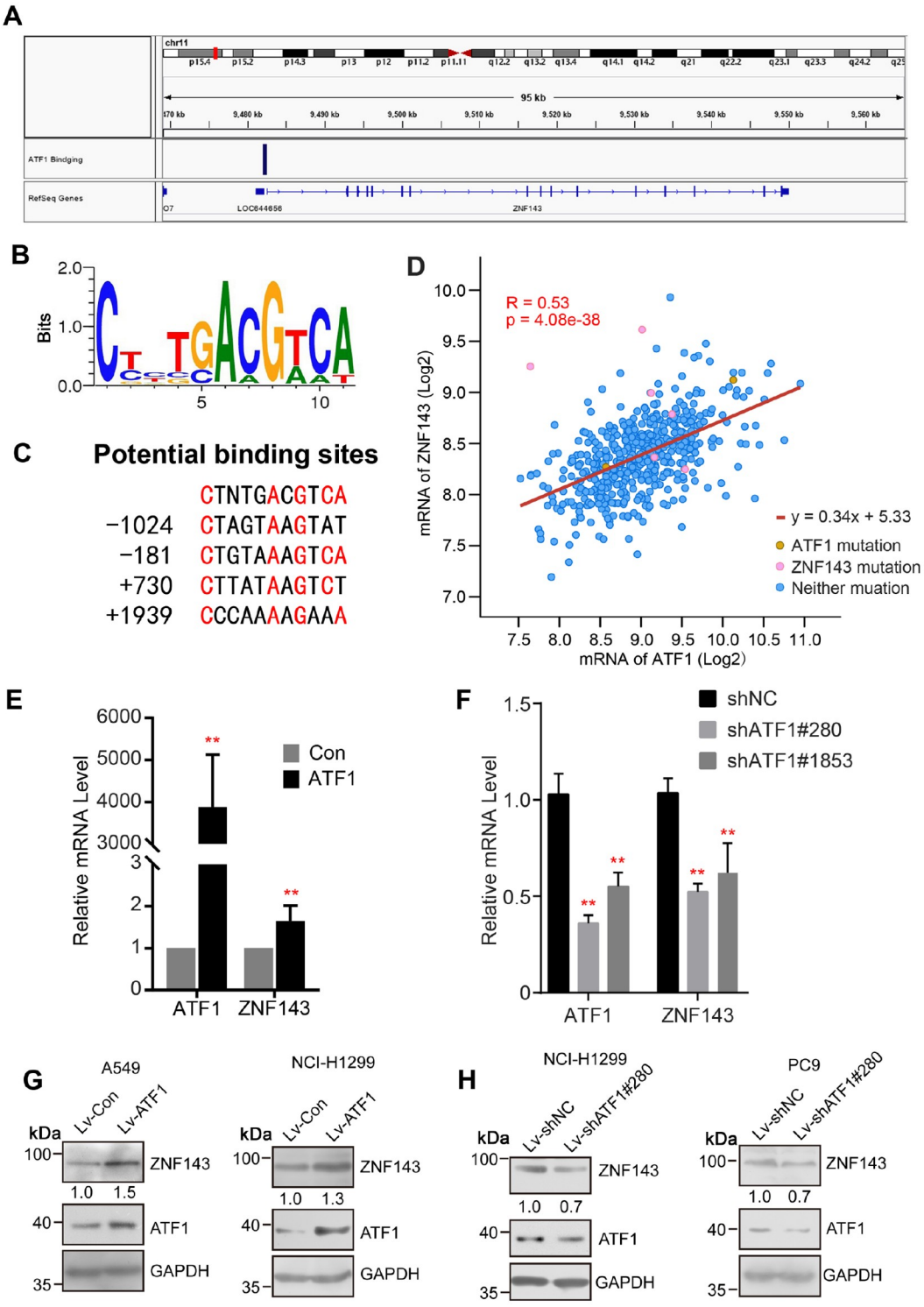

Figure 4. ATF1 transcriptionally regulates ZNF143 expression (A) ATF1 was predicted to bind to the promoter of the *ZNF143* gene in the UCSC Genome Browser database (https://genome.ucsc.edu/). (B) Consensus binding sequence for ATF1. (C) Putative transcription factor binding sites of ATF1 in the transcriptional regulation region of the *ZNF143* gene. (D) The mRNA levels of *ATF1* and *ZNF143* showed a strong correlation in lung adenocarcinoma based on analysis of data from the cBioPortal database. (E) Upregulation of ATF1 expression promoted ZNF143 expression in lung adenocarcinoma cells. NCI-H1299 cells overexpressing ATF1 or control cells were subject to detection of *ZNF143* expression by real-time PCR. (F) *ATF1* knockdown inhibited the expression of ZNF143 in lung adenocarcinoma cells. NCI-H1299 cells were transfected with shATF1#280 and shATF1#1853 to downregulate ATF1 expression, and these cells were used to determine the expression of ZNF143 by real-time PCR. (G) ATF1 overexpression enhanced the expression of ZNF143 in A549 and NCI-H1299 cells, as detected by western blot analysis. (H) Downregulation of ATF1 expression decreased the level of ZNF143 in NCI-H1299 and PC9 cells, as determined by western blot analysis. Data are presented as the mean ± SD. $^{**}P < 0.01$.

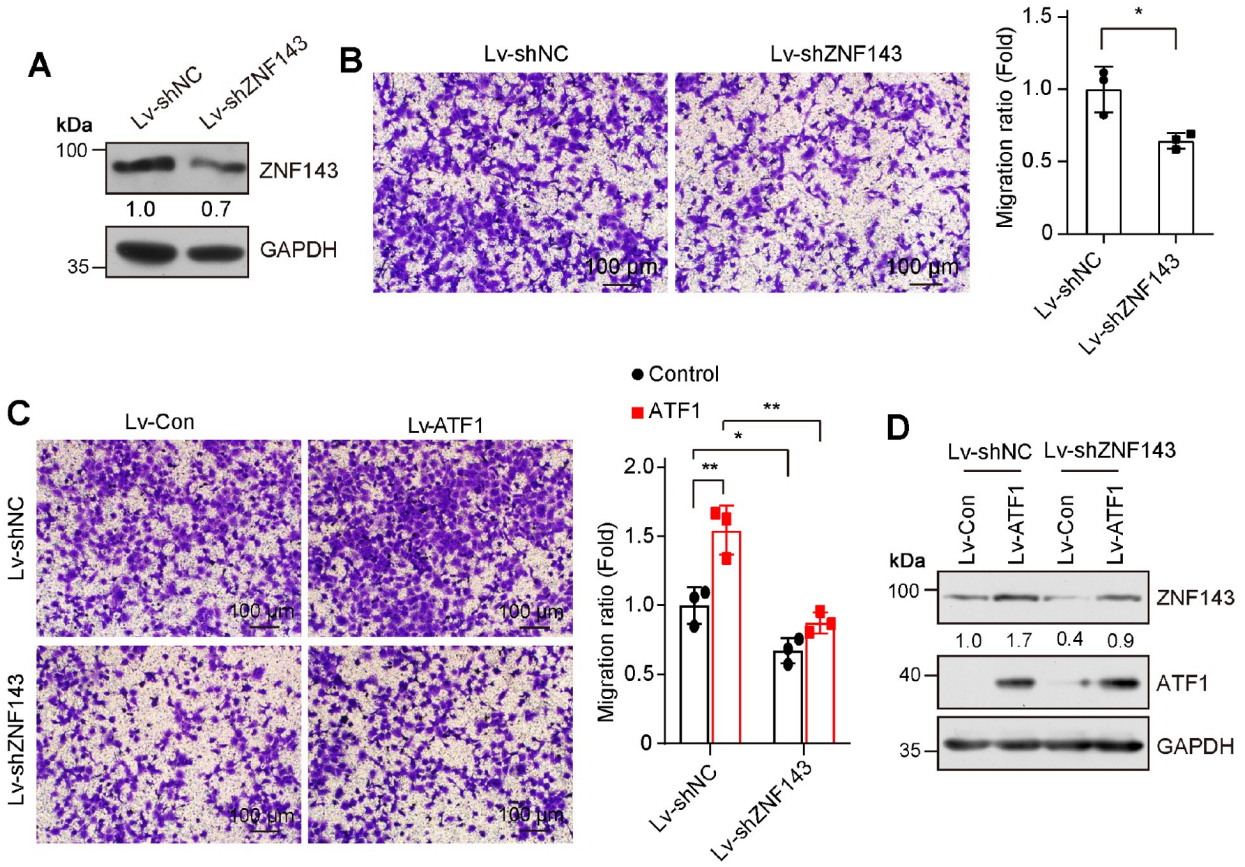

Figure 5. ATF1 promotes lung adenocarcinoma cell migration by regulating ZNF143 expression (A) ZNF143 was stably knocked down in NCI-H1299 cells. NCI-H1299 cells were infected with control (Lv-shNC) orZNF143 (Lv-shZNF143) knockdown lentivirus, and ZNF143 expression was detected by western blotting analysis. (B) *ZNF143* knockdown suppressed the migration of NCI-H1299 cells. Quantification of the cell migration ratio. (C) Downregulation of ZNF143 expression inhibited the ATF1-mediated increase in cell proliferation. (D) The expressions of ATF1 and ZNF143 were detected in cells that were used in (C). Data are presented as the mean ± SD. $*P < 0.05$, $**P < 0.01$.

migration (Figure 5C). The expression of ZNF143 in Lv-shNC and Lv-shZNF143 cells overexpressing ATF1 was detected by western blot analysis (Figure 5D). These results indicated that ATF1 promotes the migration of lung adenocarcinoma cells by transcriptionally enhancing ZNF143 expression.

Overexpression of ATF1 promotes the growth of lung adenocarcinoma cells *in vivo*

To investigate whether ATF1 is involved in the growth of lung adenocarcinoma cells *in vivo*, we generated xenograft tumor models using ATF1-overexpressing A549 cells and corresponding control cells that were generated above. These cell lines expressing ectopic ATF1 (Lv-ATF1) and the control (Lv-Con) cells were subcutaneously injected into the flanks of Balb/c-nu mice. As shown in Figure 6A–C, upregulation of ATF1 expression led to an increase in both tumor volume and weight compared with the control group. The IHC results demonstrated that overexpression of ATF1 enhanced the expression level of ZNF143 (Figure 6D). Ki67 (a well-known marker for cell proliferation) and MMP7 and MMP9 (invasion- and migration-related genes) expression levels were increased in ATF1-overexpressing tumors (Figure 6D). Taken together, these results indicated that ATF1 plays a critical role in promoting the growth of xenograft lung adenocarcinoma tumors by enhancing the expression of ZNF143 *in vivo*.

ZNF143 correlates with ATF1 in lung adenocarcinoma tissues

Considering that ATF1 transcriptionally regulates ZNF143 expression, we further determined the correlation between ATF1 and ZNF143 in lung adenocarcinoma tissues. As shown in Figure 7A–C, compared to the adjacent normal tissues, ZNF143 was highly expressed in lung adenocarcinoma tissues. High expression of ZNF143 was strongly correlated with tumor cell differentiation ($P < 0.001$) and distant invasion ($P = 0.035$) (Table 1). The expressions of ZNF143 and ATF1 showed a positive correlation in lung adenocarcinoma tissues, whereas the expressions of ZNF143 and ATF1 were not correlated in adjacent normal tissues (Figure 7D). Univariate and multivariate analyses were used to evaluate the factors associated with the recurrence and survival of lung adenocarcinoma patients, and the results showed that high expression of ZNF143 was associated with disease recurrence (Table 2). We further analyzed the relationship of the expression level of ZNF143 with the survival rate of patients with lung adenocarcinoma using the Kaplan-Meier method. The results demonstrated that lung adenocarcinoma patients with high ZNF143 expression had poor disease-free survival rates, whereas the ZNF143 expression level had no effect on overall survival in our clinical cohort (Figure 7E,F). By analyzing TCGA and GEO datasets, we found that lung adenocarcinoma patients with higher expression

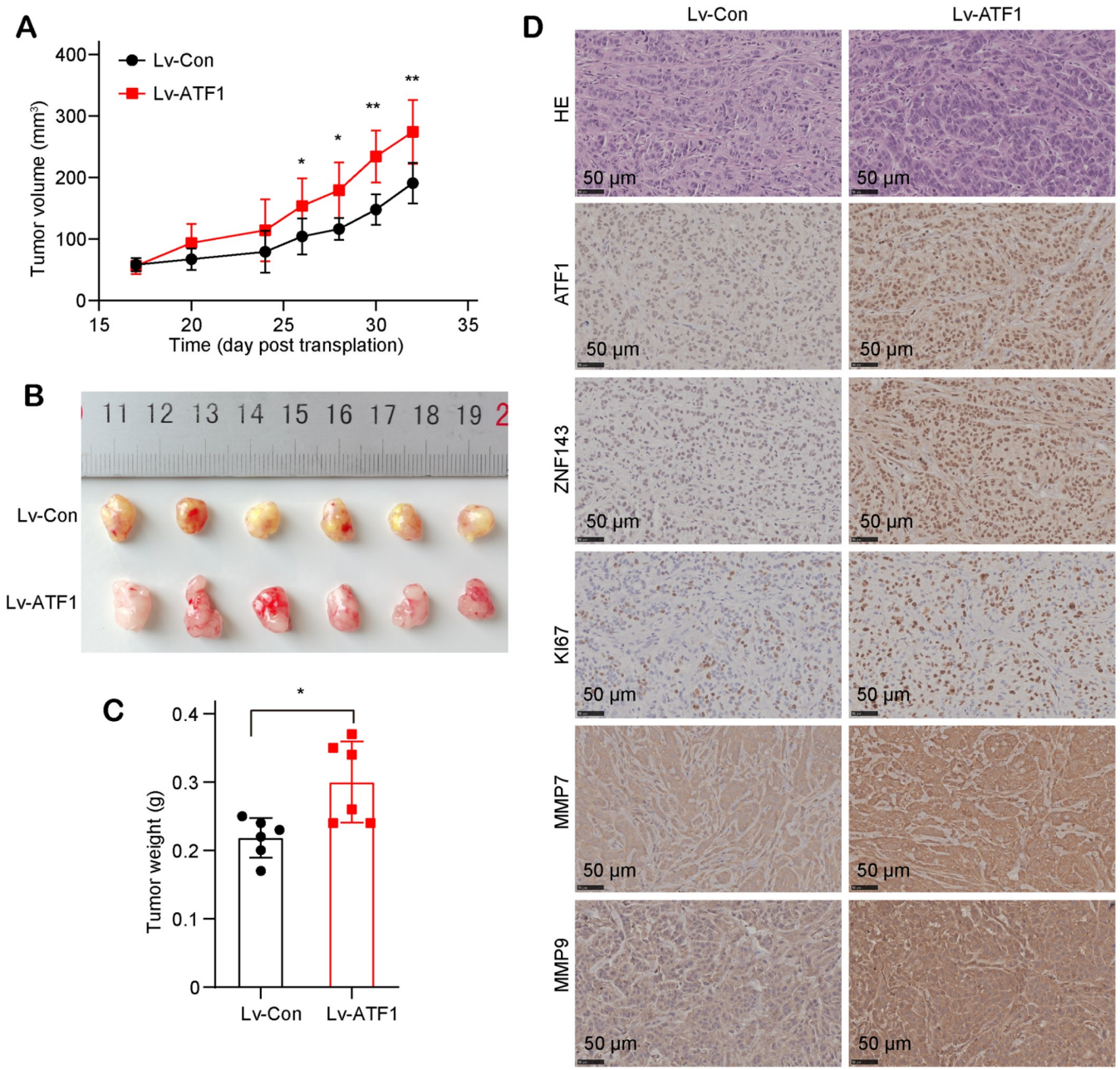

Figure 6. Upregulation of ATF1 promotes the growth of lung adenocarcinoma cells *in vivo* Upregulation of ATF1 accelerated the xenograft tumor growth of A549 cells. (A) The volumes of xenograft tumors were determined. (B) An image of the xenograft tumor is shown. (C) The weight of xenograft tumors was quantified. (D) The expressions of ZNF143, Ki67, MMP7, and MMP9 were increased in ATF1-overexpressing xenograft tumors, as detected by IHC assay. Data are presented as the mean ± SD. $*P < 0.05$, $**P < 0.01$.

of ZNF143 had shorter survival time (Figure 7G,H). Therefore, these data demonstrated that ATF1 is involved in the progression of lung adenocarcinoma by transcriptionally regulating ZNF143 expression.

Discussion

ATF1 mediates the transcriptional response to various cellular processes, including mitochondrial respiration, the heat shock response, cell survival, and cell transformation [11–14], and to various physiological and pathological processes, including early embryonic development and tumor progression [11]. ATF1 is important for cell survival during early embryonic development based on studies of the function of ATF1 using ATF1-deficient mice [11]. Cyclin-dependent kinase3 mediates the phosphorylation of ATF1 and then enhances the transcriptional activities of ATF1, regulating cell transformation [13]. An increasing number of publications have revealed that ATF1 is closely associated with the progression of various cancers [3,4,6,15–17]. The expression level of ATF1 is upregulated in T lymphomas [15], metastatic melanoma [16], colon cancer [6], hepatocellular carcinoma [17], and lung cancer [4]. Inhibiting the activation of ATF1 by using an inhibitory anti-ATF1 antibody fragment disrupted the tumorigeni-

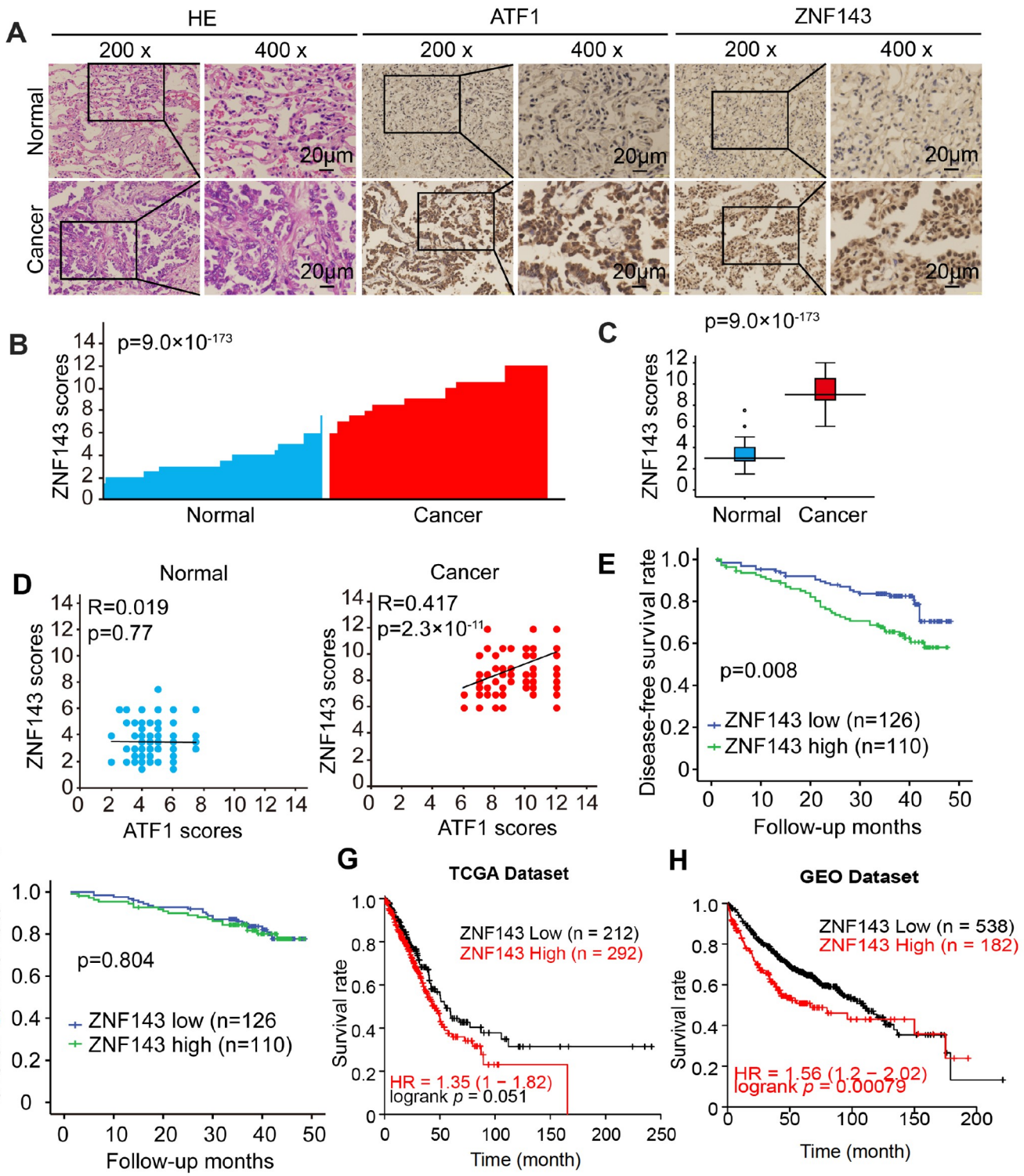

Figure 7. ZNF143 is correlated with ATF1 in lung adenocarcinoma tissues ZNF143 expression was higher in lung adenocarcinoma tissues than in adjacent normal tissues and positively correlated with ATF1 expression, as detected by IHC. (A) Representative images with magnified local images are shown. (B) Plot of the ZNF143 scores in each lung adenocarcinoma and adjacent normal tissue. (C) Box plots of the scores of ZNF143 expression in lung adenocarcinoma and adjacent normal tissues are presented. The *P* value was determined by independent-sample *t* test, $n = 236$. (D) ZNF143 and ATF1 expression levels are positively correlated in lung adenocarcinoma tissues. Spearman correlation analysis was carried out. (E) Lung adenocarcinoma patients with high ATF1 expression had a poor disease-free survival rate in our clinical cohort. The *P* values were determined by the log-rank (Mantel-Cox) test. (F) High expression of ATF1 had no significant effect on overall survival in our clinical cohort. The *P* values were determined by the log-rank (Mantel-Cox) test. (G,H) Strong expression of ZNF143 is related to poor survival of patients with lung adenocarcinoma based on analyses of data from TCGA and GEO datasets. The survival rate of patients with lung adenocarcinoma was determined by univariate analysis.

city and metastatic potential of melanoma cells in nude mice [16]. In hepatocellular carcinoma, blockade of PKA-ATF1 signaling synergized with aspirin in the inhibition of cell growth [17]. However, the oncogenic effects of ATF1 in lung cancer, especially in lung adenocarcinoma, have not been extensively characterized. In this study, we comprehensively investigated the clinical significance of ATF1 in lung adenocarcinoma and found that high ATF1 expression in lung adenocarcinoma tissues is closely related to poor prognosis (Figure 1). Consistent with a previous report [4], we found that ATF1 promoted cell migration in lung adenocarcinoma (Figures 2 and 3). The EWS (Ewing's sarcoma oncogene)-ATF1 fusion oncoprotein was reported to be strongly associated with clear cell sarcoma [7,18], but whether this fusion product is present in lung adenocarcinoma tissue and mediates lung adenocarcinoma progression is worth further investigation.

ATF1 mediates various cellular processes by transcriptionally regulating the expressions of downstream target genes. Downregulation of ATF1 expression resulted in early neuroectoderm differentiation of human embryonic stem cells by transcriptionally promoting the expression of SOX2 [19]. ATF1 acts as a key driver and activates a subset of target genes related to apoptosis and the Wnt, TGF-β, and MAPK pathways, which cooperatively increase the risk of colorectal cancer [20]. We found that ATF1 transcriptionally increased the expression of ZNF143 *in vitro* and *in vivo* (Figures 2–6). ATF1 levels were strongly correlated with ZNF143 levels in lung adenocarcinoma tissue (Figure 7). These results indicated that ATF1 promoted the malignancy of lung adenocarcinoma by specifically regulating the expression of ZNF143. However, whether other mechanisms are involved in ATF1-mediated lung adenocarcinoma progression should be further studied.

Abnormal expression of ZNF143 is involved in cancer cell proliferation, migration, and survival [8] and is associated with the progression of tumors, including hepatocellular carcinoma [21], breast cancer [22], neuroblastoma [23], glioma [24], and lung adenocarcinoma [9]. Given the important roles of ZNF143, it is considered a potential therapeutic target for tumor treatment [8,25]. Inhibition of ZNF143 activation with small molecules reduced the progression of tumors *in vitro* and *in vivo* [25]. In lung adenocarcinoma, strong expression of ZNF143 was correlated with shorter disease-specific survival [9]. We found that the expression of ZNF143 was transcriptionally regulated by ATF1, and ZNF143 regulated ATF1-mediated migration of lung adenocarcinoma cells (Figures 4–6). Our results extend the functions of ZNF143 in cancers, especially in lung adenocarcinoma.

In conclusion, we revealed a high expression level of ATF1 in lung adenocarcinoma tissues, which was associated with poor prognosis, and elucidated that ATF1 promoted lung adenocarcinoma cell proliferation and migration by transcriptionally regulating ZNF143 expression. This study provides a novel potential therapeutic target for lung adenocarcinoma and explains why ZNF143 is highly expressed in lung adenocarcinoma tissues.

Funding

This work was supported by the grants from the National Natural Science Foundation of China (No. 82060517 to L.X.) and the Natural Science Foundation of Jiangxi Province (No. 20202ACBL206032 to L.C., No. 20202BABL216045 to H.W., and No. 20212ACB206009 to M.C.).

Conflict of Interest

The authors declare that they have no conflict of interest.

References

1. Siegel RL, Miller KD, Fuchs HE, Jemal A. Cancer statistics, 2021. *CA Cancer J Clin* 2021, 71: 7–33
2. Thai AA, Solomon BJ, Sequist LV, Gainor JF, Heist RS. Lung cancer. Lancet 2021, 398: 535–554
3. Huang GL, Liao D, Chen H, Lu Y, Chen L, Li H, Li B, *et al.* The protein level and transcription activity of activating transcription factor 1 is regulated by prolyl isomerase Pin1 in nasopharyngeal carcinoma progression. *Cell Death Dis* 2016, 7: e2571
4. Cui J, Yin Z, Liu G, Chen X, Gao X, Lu H, Li W, *et al.* Activating transcription factor 1 promoted migration and invasion in lung cancer cells through regulating EGFR and MMP-2. *Mol Carcinog* 2019, 58: 1919–1924
5. Guo Y, Sun W, Gong T, Chai Y, Wang J, Hui B, Li Y, *et al.* miR-30a radiosensitizes non-small cell lung cancer by targeting ATF1 that is involved in the phosphorylation of ATM. *Oncol Rep* 2017, 37: 1980–1988
6. Huang GL, Guo HQ, Yang F, Liu OF, Li BB, Liu XY, Lu Y, *et al.* Activating transcription factor 1 is a prognostic marker of colorectal cancer. *Asian Pac J Cancer Prevention* 2012, 13: 1053–1057
7. Yamada K, Ohno T, Aoki H, Semi K, Watanabe A, Moritake H, Shiozawa S, *et al.* EWS/ATF1 expression induces sarcomas from neural crest–derived cells in mice. *J Clin Invest* 2013, 123: 600–610
8. Ye B, Yang G, Li Y, Zhang C, Wang Q, Yu G. ZNF143 in chromatin looping and gene regulation. *Front Genet* 2020, 11: 338
9. Kawatsu Y, Kitada S, Uramoto H, Zhi L, Takeda T, Kimura T, Horie S, *et al.* The combination of strong expression of ZNF143 and high MIB-1 labelling index independently predicts shorter disease-specific survival in lung adenocarcinoma. *Br J Cancer* 2014, 110: 2583–2592
10. Shao J, Xu L, Chen L, Lu Q, Xie X, Shi W, Xiong H, *et al.* Arl13b promotes gastric tumorigenesis by regulating smo trafficking and activation of the hedgehog signaling pathway. *Cancer Res* 2017, 77: 4000–4013
11. Bleckmann SC, Blendy JA, Rudolph D, Monaghan AP, Schmid W, Schütz G. Activating transcription factor 1 and CREB are important for cell survival during early mouse development. *Mol Cell Biol* 2002, 22: 1919–1925
12. Katsuyama M, Fan CY, Arakawa N, Nishinaka T, Miyagishi M, Taira K, Yabe-nishimura C. Essential role of ATF-1 in induction of NOX1, a catalytic subunit of NADPH oxidase: involvement of mitochondrial respiratory chain. *Biochem J* 2005, 386: 255–261
13. Zheng D, Cho YY, Lau ATY, Zhang J, Ma WY, Bode AM, Dong Z. Cyclin-dependent kinase 3-mediated activating transcription factor 1 phosphorylation enhances cell transformation. *Cancer Res* 2008, 68: 7650–7660
14. Takii R, Fujimoto M, Tan K, Takaki E, Hayashida N, Nakato R, Shirahige K, *et al.* ATF1 modulates the heat shock response by regulating the stress-inducible heat shock factor 1 transcription complex. *Mol Cell Biol* 2015, 35: 11–25
15. Hsueh YP, Lai MZ. Overexpression of activation transcriptional factor 1 in lymphomas and in activated lymphocytes. *J Immunol* 1995, 154: 5675–5683
16. Jean D, Tellez C, Huang S, Davis DW, Bruns CJ, McConkey DJ, Hinrichs SH, *et al.* Inhibition of tumor growth and metastasis of human melanoma by intracellular anti-ATF-1 single chain Fv fragment. *Oncogene* 2000, 19: 2721–2730
17. Zhang H, Yang S, Wang J, Jiang Y. Blockade of AMPK-mediated camp-PKA-CREB/ATF1 signaling synergizes with aspirin to inhibit hepatocellular carcinoma. *Cancers* 2021, 13: 1738

18. Komura S, Ito K, Ohta S, Ukai T, Kabata M, Itakura F, Semi K, *et al.* Cell-type dependent enhancer binding of the EWS/ATF1 fusion gene in clear cell sarcomas. *Nat Commun* 2019, 10: 3999
19. Yang SC, Liu JJ, Wang CK, Lin YT, Tsai SY, Chen WJ, Huang WK, *et al.* Down-regulation of ATF1 leads to early neuroectoderm differentiation of human embryonic stem cells by increasing the expression level of SOX2. *FASEB J* 2019, 33: 10577–10592
20. Tian J, Chang J, Gong J, Lou J, Fu M, Li J, Ke J, *et al.* Systematic Functional Interrogation of Genes in GWAS Loci Identified ATF1 as a key driver in colorectal cancer modulated by a promoter-enhancer interaction. *Am J Hum Genet* 2019, 105: 29–47
21. Zhang L, Huo Q, Ge C, Zhao F, Zhou Q, Chen X, Tian H, *et al.* ZNF143-mediated H3K9 trimethylation upregulates CDC6 by activating MDIG in hepatocellular carcinoma. *Cancer Res* 2020, 80: 2599–2611
22. Paek A, Mun J, Jo M, Choi H, Lee Y, Cheong H, Myung J, *et al.* The Role of ZNF143 in breast cancer cell survival through the NAD(P)H quinone dehydrogenase 1–p53–beclin1 axis under metabolic stress. *Cells* 2019, 8: 296
23. Tao T, Shi H, Mariani L, Abraham BJ, Durbin AD, Zimmerman MW, Powers JT, *et al.* LIN28B regulates transcription and potentiates MYCN-induced neuroblastoma through binding to ZNF143 at target gene promotors. *Proc Natl Acad Sci USA* 2020, 117: 16516–16526
24. Song Y, Shao L, Xue Y, Ruan X, Liu X, Yang C, Zheng J, *et al.* Inhibition of the aberrant A1CF-FAM224A-miR-590-3p-ZNF143 positive feedback loop attenuated malignant biological behaviors of glioma cells. *J Exp Clin Cancer Res* 2019, 38: 248
25. Haibara H, Yamazaki R, Nishiyama Y, Ono M, Kobayashi T, Hokkyo-Itagaki A, Nishisaka F, *et al.* YPC-21661 and YPC-22026, novel small molecules, inhibit ZNF143 activity *in vitro* and *in vivo*. *Cancer Sci* 2017, 108: 1042–1048